



1 Dating of an East Antarctic ice core (GV7) by high resolution 2 chemical stratigraphies

3 Raffaello Nardin¹, Mirko Severi^{1,2*}, Alessandra Amore¹, Silvia Becagli^{1,2}, Francois Burgay^{3,4}, Laura
4 Caiazzo⁵, Virginia Ciardini⁶, Giuliano Dreossi^{2,3}, Massimo Frezzotti⁷, Sang-Bum Hong⁸, Ishaq Khan³,
5 Bianca Maria Narcisi⁶, Marco Proposito⁶, Claudio Scarchilli⁶, Enricomaria Selmo⁹, Andrea Spolaor^{2,3},
6 Barbara Stenni^{2,3}, Rita Traversi^{1,2}

7 ¹Department of Chemistry “Ugo Schiff”, University of Florence, Florence, 50019, Italy

8 ²Institute of Polar Sciences of the National Research Council of Italy (ISP-CNR), 30172, Venice, Italy

9 ³Department of Environmental Sciences, Informatics and Statistics of the Ca’ Foscari University of Venice, Venice, 30172,
10 Italy

11 ⁴Laboratory of Environmental Chemistry (LUC), Paul Scherrer Institut, 5232 Villigen PSI, Switzerland

12 ⁵National Institute of Nuclear Physics (INFN), Florence, 50019, Italy

13 ⁶ENEA, Laboratory of Observations and Measures for the environment and climate, 00123 Rome, Italy

14 ⁷Department of Science, Geologic Sciences section, Roma 3 University, 00154 Rome, Italy

15 ⁸Division of Glacial Environmental Research, Korea Polar Research Institute (KOPRI), Incheon 21990, Korea

16 ⁹Department of Chemistry, Life Sciences and Environmental Sustainability, University of Parma, Parma, 43121, Italy

17

18 *Correspondence to: Mirko Severi (mirko.severi@unifi.it)

19 Abstract

20 Ice core dating is the first step for a correct interpretation of climatic and environmental changes. In this work, we release a
21 stratigraphic dating of the uppermost 197 m of the 250 m deep GV7(B) ice core (drilling site, 70°41’ S, 158°52’E, 1950 m
22 a.s.l.) with a sub-annual resolution. Chemical stratigraphies of NO₃⁻, MSA (methanesulfonic acid), non-sea salt SO₄²⁻, sea-
23 salt ions and the oxygen isotopic composition ($\delta^{18}\text{O}$) were used in the annual layer counting upon the identification of a
24 seasonal profile in their records. Different procedures were tested and thanks to the volcanic history of the core, obtained in
25 previous works, an accurate age-depth correlation was obtained for the period 1179-2009 CE. Once the dating of the core
26 was finalized, the annual mean accumulation rate was evaluated throughout the analyzed 197 m of the core, obtaining an
27 annually resolved history of the snow accumulation on site in the last millennium. A small, yet consistent, rise in
28 accumulation rate was found for the last 830 years since the middle of the 18th century.

29 1 Introduction

30 Ice cores represent remarkable natural archives able to provide paleoclimatic and paleoenvironmental information, and their
31 study is of high relevance in order to improve our understanding of the climate system. Ice cores are to this day one of, if not
32 the most, valuable archive to obtain long term, highly resolved records of the atmospheric composition and of the



33 temperatures of the past, spanning from few years up to hundreds of thousands of years (Abram et al., 2013; Delmonte et al.,
34 2002; Fischer et al., 2007; Traversi et al., 2012; Watanabe et al., 1999; Wolff et al., 2010). Antarctica and the surrounding
35 ocean play a critical role in climate dynamics (Bertler et al., 2011), but despite the huge efforts of international programs
36 (e.g., ITASE, EAIIST), a large part of the Antarctic ice sheet is still unexplored and additional cores are needed to properly
37 reconstruct the past climate and to incorporate this information in climate modeling simulations. In particular, the last
38 millennium is a critical time frame for putting the more recent human related climate change into a longer temporal context
39 and to disentangle natural versus human impacts on climate variability, but it is still poorly investigated, particularly in
40 Antarctica. New ice core records from Antarctica are needed for a better assessment of the surface mass balance (SMB) of
41 the Antarctic continent, which is highly relevant to understand its role in sea-level rise in recent decades and in the near
42 future (DeConto and Pollard, 2016; Krinner et al., 2007). Spatial coverage of climatic observation in Antarctica and the
43 Southern Ocean is still poor (Jones et al., 2016; Neukom et al., 2018) and ice core records have the potential to investigate
44 past SMB beyond the instrumental and satellite period. Recently, Thomas et al., (2017) investigated the Antarctic snow
45 accumulation variability over the last millennium at regional scale using a large number of ice core snow accumulation
46 records, grouped and assigned to different regional Antarctic areas and compared with modeled SMB.

47 In the framework of the PNRA project “IPICS – 2kyr-IT”, representing the Italian contribution to the project “The IPICS 2k
48 Array: a network of ice core climate and climate forcing record for the last two millennia”, the latter being one of the four
49 topics of the International Partnerships in Ice Core Sciences (IPICS), several drillings have been carried out in the Oates
50 Coast, East Antarctica. In this framework the site named GV7 (Figure 1) was chosen to retrieve ice cores covering at least
51 1000 yr of climatic and environmental history of this area of Antarctica. The drillings were accomplished through a bilateral
52 Italy – South Korea collaboration, during the 2013/2014 Antarctic summer.

53 One of the most critical aspect of the study of the ice core records is the dating of each ice layer, which is fundamental to put
54 the records into a temporal scale. Different methods were developed since the second half of the last century (Hammer,
55 1980) including the identification of seasonal pattern in chemical and physical stratigraphies (Alley et al., 1997; Cole-Dai et
56 al., 1997; Extier et al., 2018; Sigl et al., 2016), ice flow models and identification of temporal horizons such as volcanic
57 eruptions that brings spikes in the acidity of an ice layer and/or trace elements concentration (Castellano et al., 2005; Igarashi
58 et al., 2011).

59 Here, we focused on the identification of seasonal patterns in the ionic and isotopic composition of the core, the latter being
60 one of the most reliable and extensively used method used to date many ice cores. Since $\delta^{18}\text{O}$ in falling snow varies with
61 seasons (Dansgaard, 1964), showing maxima in summer and minima in winter, it is possible to identify an annual cycle in
62 $\delta^{18}\text{O}$ which is useful in the dating of a core. A similar annual pattern with either summer or winter maxima is found in both
63 major sea salt and non-sea salt ions found in ice cores. Both methanesulphonic acid (MSA), nitrate and the non-marine
64 fraction of the sulphate (nssSO_4^{2-}) have a seasonal pattern that could be used in the ice core dating (Pasteris et al., 2014;
65 Piccardi et al., 1994; Stenni et al., 2002; Udisti, 1996). MSA and nssSO_4^{2-} mainly arise from the atmospheric oxidation of
66 their precursor dimethyl sulfide (DMS), which in turn is produced by metabolic activities of marine phytoplanktonic species



67 (Stefels et al., 2007). The strong seasonality of DMS production leads to an analogous seasonal behavior of nssSO_4^{2-} and
68 MSA with the highest concentration peaks during the phytoplanktonic bloom, occurring in austral spring-summer
69 (November-March) (Becagli et al., 2012).
70 Unlike MSA, which only arises from marine DMS (Gondwe et al., 2003), nssSO_4^{2-} is formed also from the oxidation in
71 troposphere of SO_2 (Delmas et al., 1985), emitted during explosive volcanic eruptions, to sulphuric acid. Such acid
72 components thanks to tropospheric and stratospheric circulation (Delmas et al., 1985) could deposit in the Polar regions
73 during a period of 2-3 years after the event (Sigl et al., 2015) and their signal is superimposed over the biogenic background
74 of the nssSO_4^{2-} . The identification of such volcanic signatures in ice core records is commonly used to synchronize ice core
75 timescales (Severi et al., 2007, 2012; Winski et al., 2019) and widely used to assign an absolute date to ice layers in a core
76 (Castellano et al., 2005; Sigl et al., 2013) in conjunction with the annual layer counting.
77 The same seasonality (with a maximum in the austral summer) is also noticeable in the nitrate concentration throughout the
78 year. As one of the most abundant ions found in the cores (Legrand et al., 1999), nitrate is considered the final sink of
79 atmospheric NO_x and thanks to its role and how it interacts with the main oxidant cycles in the atmosphere is considered one
80 of the potential markers to reconstruct the oxidizing capacity of the past atmosphere (Dibb et al., 1998; Hastings et al.,
81 2005). These oxidizing processes, combined with the photochemical ones, occur more intensely during summer (Erland et
82 al., 2013; Grannas et al., 2007) and lead to a seasonal behavior of this marker as found in polar records (Stenni et al., 2002;
83 Wolff, 1995). Such clear annual cycles have been used as components of the layer-counted dating of ice cores (Wolff, 2013)
84 from both hemispheres (Rasmussen et al., 2006; Thomas et al., 2007). Since major sea-salt ions show late winter maxima in
85 their concentrations in the innermost regions of Antarctica (Udisti et al., 2012) due to large influx of sea salt aerosol during
86 winter months (Bodhaine et al., 1986), their chemical stratigraphies too could be used for the dating of the core. The same
87 summer minimum and winter-spring maximum pattern was observed at coastal stations (Mulvaney and Wolff, 1994; Weller
88 et al., 2011) and Na^+ and Mg^{2+} stratigraphies were successfully used in the dating of ice cores (Herron and Langway, 1979;
89 Winski et al., 2019). Here we present the dating of the uppermost 197 m of the 250 m deep ice core collected at GV7,
90 focusing on the interpretation of ionic stratigraphies of the core and investigating which one could be best suitable for the
91 dating itself with support of the high resolution $\delta^{18}\text{O}$ data available for the first 38 m of the core. Volcanic tie points and
92 annual layer counting were both used in order to assign an absolute date to the layer and a relative, in-between layer, dating
93 to the ice. Different dating procedures were tested and the most reliable were used concurrently with the volcanic record.
94 Once the dating for the ice core was finalized, the snow accumulation rate at the site was evaluated.

95 **2 Materials and Methods**

96 **2.1 Sampling site**

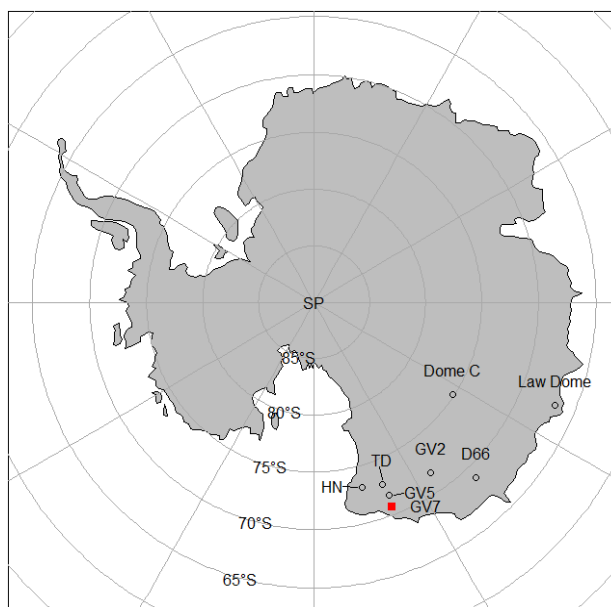
97 The GV7 drilling site is in the Oates Coast, a coastal area of the East Antarctica. The site was chosen for its relatively high
98 snow accumulation rate (241 ± 13 mm w.e. yr^{-1} over the past 50 years), the thickness of the ice (approx. 1700m), the limited



99 post depositional processes due to the reduced force of katabatic winds along the ice divide (Becagli et al., 2004; Frezzotti et
100 al., 2007; Magand et al., 2004) and the excellent stratigraphy (chemical and isotopic) (Caiazzo et al., 2017; Delmonte et al.,
101 2015; Frezzotti et al., 2007). Internal layers of strong radar reflectivity observed with ground-penetrating radar (GPR) are
102 isochronous, and surveys along continuous profiles provide detailed information on the spatial variability of snow
103 accumulation. Spatial distribution of snow accumulation from GPR layer (dated to 1905 ± 9 AD) has been conducted during
104 the 2001-2002 ITASE expedition from 150 km north of GV7 up to Talos Dome (Frezzotti et al., 2007). Spatial distribution
105 of snow accumulation from GPR layer upstream GV7 site shows that internal layering and surface elevation are continuous
106 and horizontal up to 10 km from the site, revealing low ice velocity 0.3 ± 0.01 m yr⁻¹, no distortion of isochrones due to ice
107 flow dynamics and very low snow accumulation spatial variability (less than 5%, Frezzotti et al., 2007). An extensive
108 chemical dataset covering 7 years of deposition on site obtained from the analysis of two snow pits is already available
109 (Caiazzo et al., 2017), as well as an in-depth reconstruction of the past volcanic history (Nardin et al., 2020).

110 2.2 Fieldwork

111 During the 2013/14 Antarctic campaign, six shallow firn cores (5 to 50 m) and two intermediate firn-ice core (87 and 250 m
112 deep) were retrieved. The 250 m deep core (named GV7(B)) is the object of this work. The drilling of the ice core (see Figure
113 1) was accomplished using an electromechanical drilling system (Eclipse Ice drill Instrument).



114
115 **Figure 1: GV7 (70°41'17.1'' S, 158°51'48.9'' E; 1950 m) drilling site (red square). Hercules Nevè (HN), Talos Dome (TD), GV5,**
116 **GV2, D66, Dome C and Law Dome ice cores' drilling site are also reported.**

117
118 The drilling started at 3 m from the snow surface and reached a depth of 250.2 m. Drilling fluid (Exxsol D40) was used from
119 a depth of 80 m (close off 75 m) and inserted inside the hole with a tube. A level of 4 m of fluid was found to be ideal to aid



120 the drilling operation and improved the quality ice cores. The Eclipse system has experienced problems during the drilling
121 below 100 m of depth, the brittleness of the ice, breaks in the core and the presence of drilling fluids in these cracks proved
122 to be a problem in the decontamination of the core. The presence of numerous breaks and therefore a lack in continuity of
123 the stratigraphy, prevented us to analyze the deeper part of the core and only the first 194 meters (reaching a depth of 197 m)
124 were analyzed.

125 2.3 Ice core analysis

126 60 cm long ice core sections (cut and logged directly in field) were shipped to the EUROCOLD lab of the University of
127 Milano-Bicocca (Italy) where they were cut longitudinally and transversally and distributed among different research groups.
128 The 4x4 cm core strips for ionic content analysis were sealed in plastic bags, shipped frozen to the cold room of the
129 Department of Chemistry of the University of Florence (Italy) and stored at -20°C until the moment of analysis. Conversely,
130 both the bag (60 cm) and the high-resolution samples (4 cm) for the isotopic analysis were melted at room temperature and
131 transferred in 25 mL HDPE bottles at the EUROCOLD lab and then sent to the Ca' Foscari University of Venice and the
132 University of Parma for the isotopic measurements.

133 The strips for ionic content were manually decontaminated inside the cold room of the Department of Chemistry of the
134 University of Florence (Italy), by scraping the outermost layer of ice (approx. 1 cm) using ceramic knives to remove external
135 contamination (Candelone et al., 1994; Chisholm et al., 1995; Tao et al., 2001, Caiazza et al., 2016).

136 All decontamination procedures were carried on under a class-100 laminar flow hood and the sub samples were stored inside
137 pre-cleaned plastic vials and analyzed within a week to avoid external contamination. For those sections of the ice core too
138 badly damaged to be manually decontaminated (due to problems in the drilling operations, handling and fracturing of the
139 ice), the fractures were logged, and the sample decontaminated just before the analysis by quickly submerging it three times
140 (10 seconds the first wash then 5 seconds the remaining two) in ultra-pure Water (18.2 MΩ 25°C) in order to remove the
141 outer layer of ice. Each sub-sample was melted at room temperature under laminar flow hood just before the analysis. The
142 sub-samples were then analyzed for ionic content using two Ion Chromatograms operating simultaneously: a Thermo Dionex
143 ICS-1000 for the determination of the cationic content (Li⁺, Na⁺, NH₄⁺, K⁺, Mg²⁺, Ca²⁺) and Thermo Dionex DX-500
144 equipped with a GP50 gradient pump for anionic content (F⁻, Formate, methanesulfonate (MS⁻, referred in the text as MSA),
145 Cl⁻, NO₃⁻, SO₄²⁻). Further details about the columns used and the daily calibration procedures for each ion chromatographic
146 system are described in (Caiazza et al., 2016; Morganti et al., 2007), while the analytical performance of the methods were
147 tested and described in (Nardin et al., 2020).

148 Samples for isotopic analysis did not require any decontamination procedure. Bag samples (60 cm) were analyzed for δ¹⁸O at
149 the University of Parma, using a Thermo-Fisher Delta Plus Isotope-ratio Mass Spectrometer (IRMS) coupled with a HDO
150 automatic equilibration device, following the classical water-CO₂ equilibration technique described by Epstein and Mayeda,
151 (1953). High resolution samples (4cm) were analyzed for δ¹⁸O at the Ca' Foscari University of Venice, using both the IRMS
152 water-CO₂ equilibration technique (Thermo-Fisher Delta Plus Advantage coupled with a HDO automatic equilibration



153 device) and the Cavity Ring-down Spectroscopy (CRDS) technique (Picarro L1102-I). The Thermo-Fisher Delta Plus and
154 the Delta Plus advantage are both characterized by an analytical precision of 0.05‰ for $\delta^{18}\text{O}$, while the Picarro L1102-I has
155 an analytical precision of 0.10‰ for $\delta^{18}\text{O}$. All measurements were calibrated using internal isotopic standards periodically
156 calibrated against the certified International Atomic Energy Agency (IAEA) standards VSMOW2 and SLAP2- All the
157 isotopic data are reported in the SMOW-SLAP δ -scale.

158 2.4 Major ions contribution

159 Chemical stratigraphies of the relevant ions for the dating procedure were obtained by plotting the concentration (in $\mu\text{g/L}$)
160 against the mid depth of the sample, logged during the decontamination procedure. Minimal manipulation was done over the
161 raw dataset of the different ions' concentration, but extremely high concentration points (i.e. spikes in the concentration of a
162 single ion) were discarded and attributed to external contamination. This was done by removing all the points above the 99th
163 percentile for all the ions used in the dating procedure; this was chosen as a good compromise to keep high values of
164 concentration due to particular events (e.g., volcanic eruptions) and at the same time remove those due to possible
165 contamination. The non-sea salt sulphate (from now on referred as nssSO_4^{2-}) was calculated by equation (1)

$$166 \quad \text{nssSO}_4^{2-} = \text{totSO}_4^{2-} - 0.25 * \text{Na}^+ \quad (1)$$

167 where 0.25 is the average $\text{SO}_4^{2-}/\text{Na}^+$ ratio in sea water, totSO_4^{2-} and Na^+ are the total measured concentration of the two
168 ions respectively. We assumed that the only contribution for sodium is the sea spray aerosol (Legrand and Delmas, 1984;
169 Maupetit and Delmas, 1992). Both in inland (Röthlisberger et al., 2002) and coastal sites (Benassai et al., 2005; Nyamgerel
170 et al., 2020) the crustal contribution of sodium is found to be very low or negligible compared to the marine one. When
171 calculated for GV7 using a simple equation system (2) (Becagli et al., 2012; Udisti et al., 2012)

$$172 \quad \text{tot-Na}^+ = \text{ss-Na}^+ + \text{nss-Na}^+ \quad (2)$$

$$173 \quad \text{tot-Ca}^{2+} = \text{ss-Ca}^{2+} + \text{nss-Ca}^{2+}$$

$$174 \quad \text{ss-Na}^+ = \text{tot-Na}^+ - 0.562 \text{nss-Ca}^{2+}$$

$$175 \quad \text{nssCa}^{2+} = \text{tot-Ca}^{2+} - 0.038 \text{ss-Na}^+$$

176 where 0.562 and 0.038 represent the $\text{Na}^+/\text{Ca}^{2+}$ w/w ratio in the crust (Bowen, 1979) and seawater (Nozaki, 1997),
177 respectively; the non-sea salt contribution of Na^+ was found to be 3% as average, lower than the analytical error for ions
178 determination.

179 The nssSO_4^{2-} was used in the identification of volcanic signatures in the GV7 ice core using already established methods
180 (Castellano et al., 2004, 2005; Sigl et al., 2013; Traufetter et al., 2004) on Arctic and Antarctic ice cores, here briefly
181 described. The biogenic background was calculated as the running average of the nssSO_4^{2-} concentrations and its standard
182 deviation (σ) was used to set the threshold over which a sample point was to be attributed to a volcanic eruption. Both 2σ



183 and 3σ were used as thresholds added to the average biogenic background as described more in details in Nardin et al.,
184 (2020) where an in-depth discussion of the volcanic fluxes of the volcanic eruptions found in the core is also present.

185 **2.5 Trace element analysis**

186 The ice samples were analyzed with an Inductively Coupled Plasma Single Quadrupole Mass Spectrometer (ICP-qMS,
187 Agilent 7500 series, USA) equipped with a quartz Scott spray chamber. A 120-seconds rinsing step with 2% HNO₃
188 (Suprapure, Romil, UK) was performed after each sample to limit any possible memory effect, the vials used for standard
189 preparation were cleaned following the same procedure adopted for ice samples. The ²⁰⁹Bi, ²⁰⁵Tl and ²³⁸U quantification was
190 performed using external calibration curves with acidified standards (2% HNO₃, Suprapure, Romil, UK) from dilution of
191 certified IMS-102 multielemental standard (10 ppm ± 1%, Ultra scientific). The resulting external calibration curves for the
192 three elements were 0.999. The Limit of Detection (LoD) for Tl and U was 0.001 ppb while for Bi 0.004 ppb, calculated as
193 three times the standard deviation of the blank.

194 **2.6 Trend analysis**

195 Trend analysis of the cores was based on the calculation of breakpoints between periods with significantly different trends
196 following Tomé and Miranda (2004). The methodology uses a least-squares approach to compute the best continuous set of
197 straight lines that fit a given time series, subject to a number of constraints on the minimum distance between breakpoints
198 and, optionally, on the minimum trend change at each breakpoint. We chose a period of 150 yr as minimum distance to
199 identify trend at seculars scale. The choice is subjective, but it takes into account the high computational request for too
200 small minimum distance and the risk of non-significance for too large minimum distance. Due possible noise connected to
201 local spatial variability (Frezzotti et al., 2007) at the three sites (Talos Dome, GV7 and Law Dome) we applied the procedure
202 to seven years smoothed average in order to make all the cores comparable between each other.

203 **3 Results and Discussion**

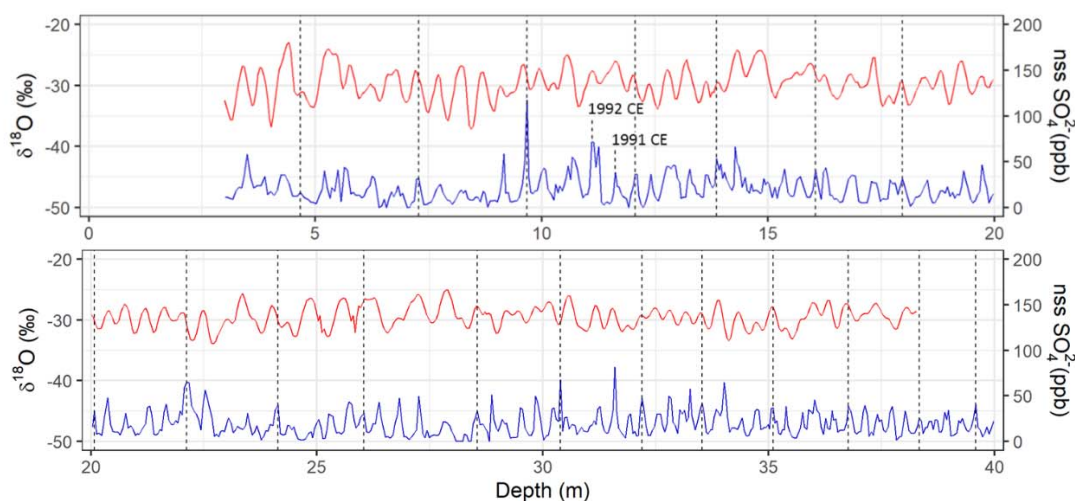
204 The relatively high snow accumulation rate on the site (well above 200 mm w.e. yr⁻¹ Frezzotti et al., 2007) allows an
205 accurate dating of the core by counting successive snow layers, identifiable by markers having seasonal pattern and/or the
206 identification of specific dated event, mainly in the form of volcanic eruptions identified in the stratigraphies as spikes of
207 nssSO₄²⁻ statistically higher than the biogenic background (Nardin et al., 2020).

208 **3.1 Ice core dating procedure – upper section**

209 The previous work on snow pit dating at the GV7 site (Caiazzo et al., 2017) revealed that nssSO₄²⁻ and δ¹⁸O stratigraphies
210 show the best seasonal pattern with summer maxima in phase between them. Therefore, for the uppermost section of the core
211 (38.27 m) for which the δ¹⁸O high resolution stratigraphy was available, two independent dating using nssSO₄²⁻ and δ¹⁸O



212 respectively were produced assigning to each local maximum of the nssSO_4^{2-} profile the date 1st of January of any given
213 year. The two records vs. depth were compared and are shown in Figure 2. In both profiles, a clear seasonal pattern can be
214 identified, and it was used to accurately date the first 40 m of the core. Minor discrepancies between the two profiles are to
215 be expected and are probably due to the slightly different depth resolution of the two series (4.5 cm and 4 cm on average for
216 nssSO_4^{2-} and $\delta^{18}\text{O}$, respectively).

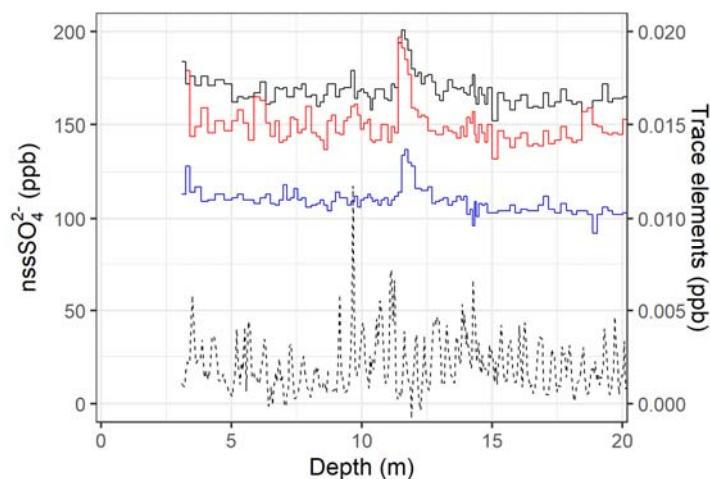


217
218 **Figure 2: $\delta^{18}\text{O}$ (red, left scale) and nssSO_4^{2-} (blue, right scale) profiles against depth used in the dating of the uppermost 40 m of**
219 **the GV7 core. Vertical dashed lines represent intervals of 5 years starting at Year 2005 CE at a depth of 4.67m**

220 In order to constrain the dating and assign an absolute date to the layer, two volcanic signatures were found in the time
221 period investigated: 1992 Pinatubo eruption (found at a depth of approx. 11.1 m) and 1964 Agung volcanic eruption (found
222 at a depth of approx. 22.1 m). As discussed in previous work, neither of these volcanic eruptions display a strong signal in
223 the nssSO_4^{2-} in the GV7 core and trace element stratigraphies were used to constrain the 1992 CE tie point identification.
224 Trace elements deposition in polar ice cap is mainly associated with dust deposition. Evidence for anthropogenic
225 contribution in the global trace elements deposition is well documented, such as the increase in lead depositional flux in
226 connection with the introduction of lead containing gasoline. Specific trace elements such as Tl and Bi have been proposed
227 to be enriched in deposition derived from volcanic eruption (Candelone et al., 1995; Kellerhals et al., 2010). Bi, Tl and U
228 show an increased concentration between 11.0 and 12.5 m depth (Figure 3), corresponding with the 1989-1992 CE time
229 period, according to the $\delta^{18}\text{O}$ annual layer counting dating. Bi, Tl and U concentrations peaks, to be attributed to the 1991
230 CE Cerro Hudson and/or the 1991 CE Pinatubo eruption, are recorded at a higher depth compared to the nssSO_4^{2-} and the
231 deposition of sulphuric compounds for these eruptions in the Antarctic plateau occurs mainly in the year 1992 CE. However,
232 dust (and therefore trace elements) deposition occurs earlier, as reported by Hwang et al. (2019) analyzing the same volcanic
233 eruption from snow pits drilled near Dome Fuji in Dronning Maud Land, hence further consolidating the date attribution to
234 the trace elements and nssSO_4^{2-} concentration's spikes in this work (1992 CE). Therefore, the uppermost section of the core



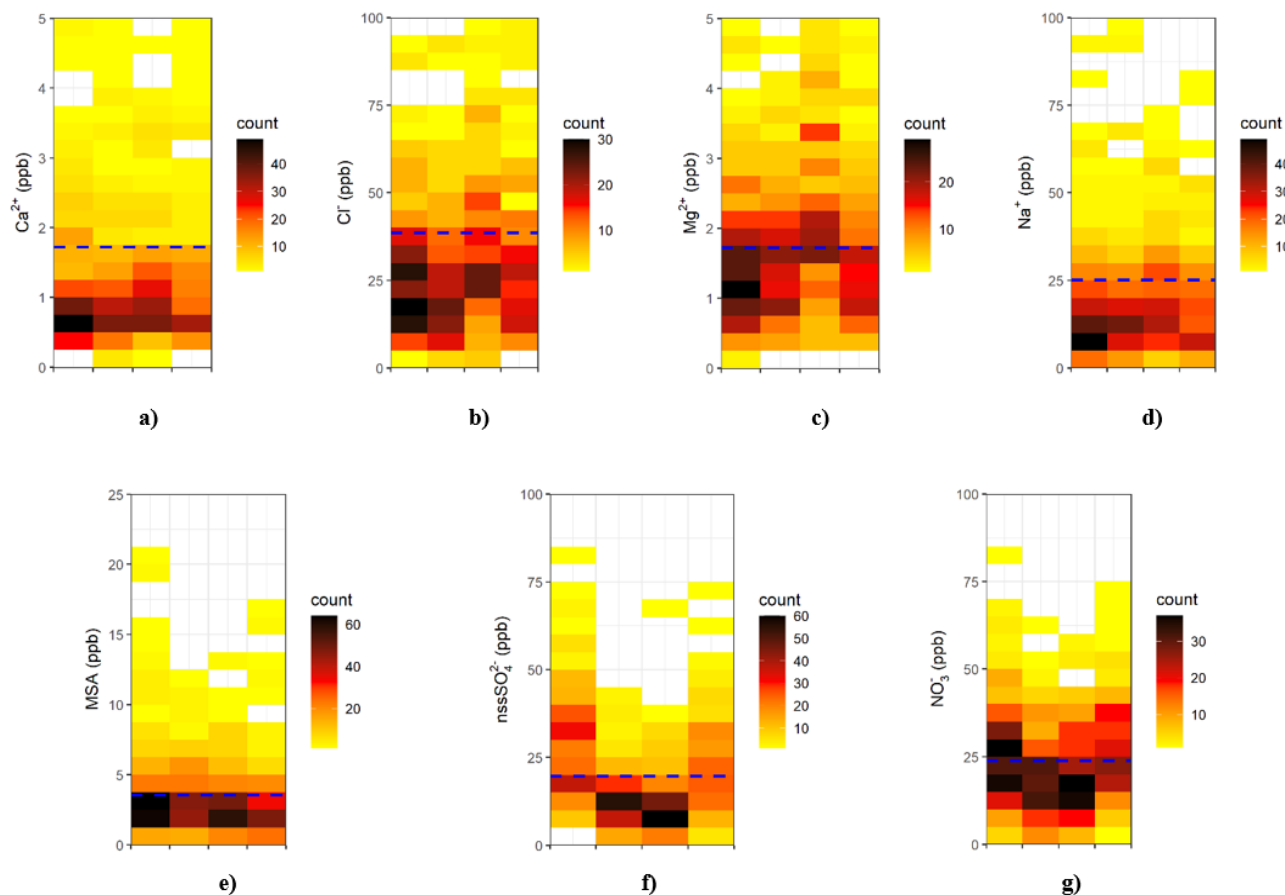
235 (3.00 to 38.27 m) was dated and was found to cover the time period 2009-1920 CE. The uncertainty of this dating is
236 discussed further below.



237
238 **Figure 3: comparison of the nssSO_4^{2-} (dashed line, left scale) and Tl, Bi, U (black, red and blue line respectively, right scale)**
239 **stratigraphies for the first 20 m of the GV7 ice core**

240 3.2 ice core dating procedure – lower section

241 Due to the lack of high-resolution data for $\delta^{18}\text{O}$ for the deeper part of the core, only ion signatures could be used for the
242 dating of the rest of the core. In order to highlight the seasonal character of each ion and to decide whether or not some ions
243 are more useful than others for the GV7 ice core dating, we considered the concentration profile of each ion throughout the
244 89 years already dated in the above section. Each year was equally divided in 4 parts corresponding to the Antarctic seasons
245 and roughly to the time periods January-March, April-June, July-September and October-December. It has been noticed that
246 the equal division in four time periods is an approximation as snow deposition is not constant throughout the year in the
247 coastal regions of Antarctica but considering a dataset of more than 700 sample points spanning a time period of 89 years
248 this approximation can be acceptable. By dividing each year in just four intervals, we were able to understand which ion(s)
249 showed the more pronounced seasonal pattern in the core by using bin plots (Figure 4). Both winter and summer maxima are
250 usable for the annual layer counting procedure. When comparing the profile of each ion to the average calculated in the
251 considered time interval, both sea-salt ions (Cl^- , Mg^+ and Na^+) and non-sea salt ones (NO_3^- , nssSO_4^{2-}) showed a maximum
252 throughout the year, but as shown in Figure 6, the more pronounced one was the one of the nssSO_4^{2-} with most of the lower
253 concentration points in the 5-10 $\mu\text{g/L}$ bin (middle of the year) and most of the higher concentration points in the 35-40 $\mu\text{g/L}$
254 bin (beginning of the year). Sea-salt ions showed winter maxima, and especially the Mg^{2+} profile (Figure 6 c), with generally
255 higher values of concentration (up to 3.5 $\mu\text{g/L}$ compared to an average of 1.71 $\mu\text{g/L}$), but in general the most populated bins
256 in the winter and summer periods showed similar concentrations, suggesting a lack of a pronounced seasonal pattern that
257 could be helpful in the dating procedure.



258

259 **Figure 4: Seasonal variability of sea-salt ions (Ca^{2+} (a), Cl^- (b), Mg^{2+} (c), Na^+ (d) and non-sea-salt ions (MSA (e), nssSO_4^{2-} (f), NO_3^-**
260 **(g) found in the GV7(B) ice core. Concentration's bin are 3 “months” in width and 5 ppb in height except for MSA levels (1 ppb)**
261 **and Calcium and Magnesium (0.25 ppb). Upper concentration limits and bin sizes were chosen to keep between each ion's plot the**
262 **same proportions in order to facilitate the interpretation of the data. In blue, the average concentration of each ion in the time**
263 **interval investigated.**

264 These considerations only cover a small section of the core (approx. the 20% of its length and due to the compression of the
265 snow and the ice layers, reasonably even less so when considering the time period investigated with this core), but as shown
266 in Figure 5, nor the Na^+ nor the Mg^{2+} concentration vs. depth profile seem to show a clear and usable annual pattern at
267 greater depths of the core and not always a maximum in the nssSO_4^{2-} concentration coincide with a minimum in the other
268 two ions concentration. This lack of anticorrelation was further highlighted when a principal component analysis (PCA) was
269 performed on the whole dataset of concentrations measured in the core: by doing so the n-dimensions dataset was reduced to
270 a lower number of dimensions (Principal Components or Factors) by means of orthogonal linear correlation of the
271 interrelated variables The first PC explains the most variation of the n-dimension dataset. PCA was performed using the
272 software STATISTICA (extraction: principal components, rotation: Varimax normalized).

273 Two factors were extracted with PCA (see Table S1 and Figure S2). As expected, a strong correlation between sea-salt ions
274 was found (grouped in Factor 1), as well as a good correlation between NO_3^- and nssSO_4^{2-} levels throughout the core



275 (grouped in Factor 2). In Factor 2 NO_3^- and nssSO_4^{2-} present the highest factor loading, but they are negative, highlighting
276 the opposite seasonal pattern of the two factors: concentration maxima in winter and summer for Factor 1 and 2,
277 respectively.

278 Based on the seasonality of the ionic marker highlighted by the bin plots and PCA analysis, a number of dating procedures
279 reported in literature were checked for GV7 ice core.

280 1) Multiparametric approach using the sum of MSA, NO_3^- and nssSO_4^{2-} normalized concentrations as reported by
281 Udisti (1996). Normalization means that every concentration is divided by the values of the nearest concentration
282 maxima, in this way is possible to give the same relevance to maxima having different concentration values in the
283 same data series and from different data series.

284 2) Since by normalizing the three series (all showing similar patterns) each sample points would have the same
285 “weight” in the dating procedure; this should be useful for nearby volcanic eruptions, where the high concentration
286 of sulphate could potentially mask the seasonal pattern, but as highlighted by bin plot and PCA, MSA maxima do
287 not exactly match the other ions. For NO_3^- , its maxima can also be shifted by nearby volcanic eruptions due to the
288 high acidity from H_2SO_4 (Jiang et al., 2019; Röthlisberger et al., 2000, 2002). For these reasons, this method was
289 found not reliable in the lower section of the core as shown in Figure S3, where the different stratigraphies are
290 compared.

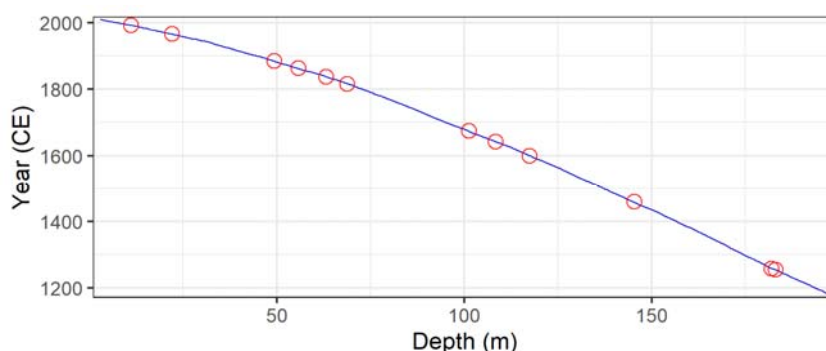
291 3) Cation stratigraphies: although Na^+ and Mg^{2+} stratigraphies were successfully used in the dating of ice cores
292 (Herron and Langway, 1979; Winski et al., 2019) for the GV7 site they showed a less pronounced seasonal pattern
293 both in the upper (as seen in the bin plots in Figure 4) and lower portions compared to the nssSO_4^{2-} profile, as in
294 Figure S4. Therefore, identification of winter maxima in their concentration profiles is not univocal, making
295 impossible the accurate core dating.

296 4) As already seen in the first section of the core from the preliminary analysis of the different ions, the dating of the
297 GV7 ice core using the nssSO_4^{2-} concentration vs. depth profile without any further data manipulation is possible
298 and the bin plot analysis suggests that this is, indeed, the best approach for dating the rest of the core.

299 The dating of the core was therefore carried out with a combination of annual layer counting and the identification of
300 volcanic signatures in the core. The know past volcanic eruptions found in other ice cores (Sigl et al., 2013, 2015, 2016;
301 Zielinski et al., 1996) as well as the tephra layer (Narcisi et al., 2001, 2012; Narcisi and Petit, 2021) and their assigned date
302 is reported in Table 1. Regardless of the exact date, due to the way the dating was finalized, the layers characterized by a
303 rising in the nssSO_4^{2-} concentration coinciding to a given eruption was assigned to the 1st of January in order to be
304 consistent with the dating of the seasonal maxima. The complete stratigraphy of the nssSO_4^{2-} is reported in Figure S5 and the
305 finalized dating in Figure 5. When it comes to annual layer counting, a rigorous evaluation of the uncertainty of the dating is
306 difficult to accomplish and it is usually estimated based on the algorithm used to identify each annual layer (Sigl et al., 2016;
307 Winski et al., 2019) and/or by taking into account the uncertainty on the dating of different ice cores used as reference



308 (Winski et al., 2019). In this work we estimated the uncertainty over the annual layer counting as the sum of the layer
 309 uncertainties highlighted in the dating procedure, estimated to be 0.5 ± 0.5 years (Ramussen et al., 2006). The uncertainty was
 310 estimated between each one of the known volcanic signatures highlighted in the ice core, dated with an uncertainty of ± 1
 311 year from the recorded eruption due to the amount of time needed to reach Antarctica.
 312 The same level of uncertainty was assigned to the missing sections of the core, where the number of years present was
 313 estimated using the average year/depth ratio calculated in 10 years before and after the break. Uncertainty levels are reported
 314 in Table 2; the relatively higher number of uncertain layers in the lower section of the core is due to missing ice that led to a
 315 non-continuous profile and to the lower resolution of the core, where each year could be represented by as low as 3 sample
 316 points. Major volcanic eruptions in this section of the core are also fewer and far between each other (see Table 1), and the
 317 lack of temporal horizon to constrain the dating, brought higher degree of uncertainty in the dating itself.



318
 319 **Figure 5: age depth correlation for the GV7(B) ice core. Temporal horizons used as constraints in the dating procedure are**
 320 **highlighted with red circles**

Volcano	Depth (m)	Historical date (start) Year (CE)	Assigned date Year (CE)
Pinatubo	11.10	1991	1992
Agung	22.12	1963	1965
Krakatoa	49.35	1883	1884
Makian	55.75	1861	1863
Cosiguina	63.27	1835	1837
Tambora	68.75	1815	1816
Gamkonora	101.25	1673	1675
Parker Peak	108.39	1641	1642
Huaynaputina	117.48	1600	1600
Reclus?	145.41	1460	1460



Samalas	181.86	1257	1258
Tephra Layer	183.07	1253	1254

Table 1: known past volcanic eruptions used in the dating of the core

GV7 section (m)	Number of Annual Layers		Duration (yrs)	Counting Error	
	Certain	Uncertain		Absolute (yrs)	Percentage
3.00 – 11.10	17	0	17	-	-
11.10 - 22-12	26	1	27	0.5	1.9
22.12 – 49.35	76	5	81	2.5	3.1
49.35 – 55.75	21	1	22	0.5	2.3
55.75 – 63.27	24	3	27	1.5	5.6
63.27 – 68.75	18	3	21	1.5	7.1
68.75 – 101.25	136	5	141	2.5	1.7
101.25 – 108.39	31	1	32	0.5	1.6
108.39 – 117.48	37	4	41	2	4.9
117.48 – 145.41	133	9	142	4.5	3.2
145.41 – 181.86	188	12	200	6	3.0
181.86 – 183.07	4	0	4	-	-
183.07 – 197.00	69	6	75	3	4.0

Table 2: Uncertainty levels over the GV7 ice core dating

3.3 Mean Snow Accumulation Rate evaluation

Once the dating was finalized, for each year the amount of annual snow accumulated on the site was calculated in millimeter of water equivalent per year (mm w.e. yr⁻¹) by multiplying the length of the core representative of any given year by the density of the core itself. The density (in g cm⁻³, see Figure S4) was evaluated by weighting each section of the core.

Caiazza et al. (2017) dating of a snow-pit by chemistry seasonal signal reports a mean accumulation rate of 242 mm w.e. yr⁻¹ for the period 2008-2013 CE with a Standard Deviation (SD) of 71 mm w.e. yr⁻¹, value very close to the estimation of the accumulation of the previous 50 years made by Magand et al., (2004) using atomic bomb horizon marker (241 ± 13 mm w.e. yr⁻¹ from 1965 to 2000 CE). Frezzotti et al. (2007) report an accumulation of 252 mm w.e. yr⁻¹ for the period 2001-2004 CE with a SD of 104 mm w.e. yr⁻¹ using snow stakes farm measurements and a mean accumulation of 237 mm w.e. yr⁻¹ for the



336 period 1854–2004 CE using the seasonal variation in nssSO_4^{2-} concentrations, coupled with the identification of atomic bomb
337 markers and nssSO_4^{2-} spikes from the most important past volcanic event.

338 The mean GV7(B) accumulation for periods 1965–2000 CE and 1854–2004 CE (242 with SD of 57 mm w.e. yr^{-1} and 233
339 with SD of 64 mm w.e. yr^{-1} , respectively) confirm the ones found in the snow pits, stake measurements and shallow ice core
340 previously analyzed and covering different period during the last 150 years. On the other hand, the mean snow accumulation
341 calculated from the totality of the 195 m, representative for a time period ranging between and 1179 and 2009 CE, is 205
342 mm w.e. yr^{-1} (SD of 63 mm w.e. yr^{-1}) lower than the one previously measured for the last century.

343 The comparison between GV7(B) and the ITASE record (Figure 6) highlights a similar trend especially in the period ranging
344 from 1900 to 2001 CE where the linear correlation between the two cores is high and significant ($R=0.42$, $p<0.0001$). On the
345 other hand, if we consider also part of the 18th century, the correlation decreases ($R=0.3$ $p<0.0002$) due to few
346 inconsistencies apparent between 1880 and 1850 CE probably due to the dating of the two cores, based on different spatial
347 sampling.

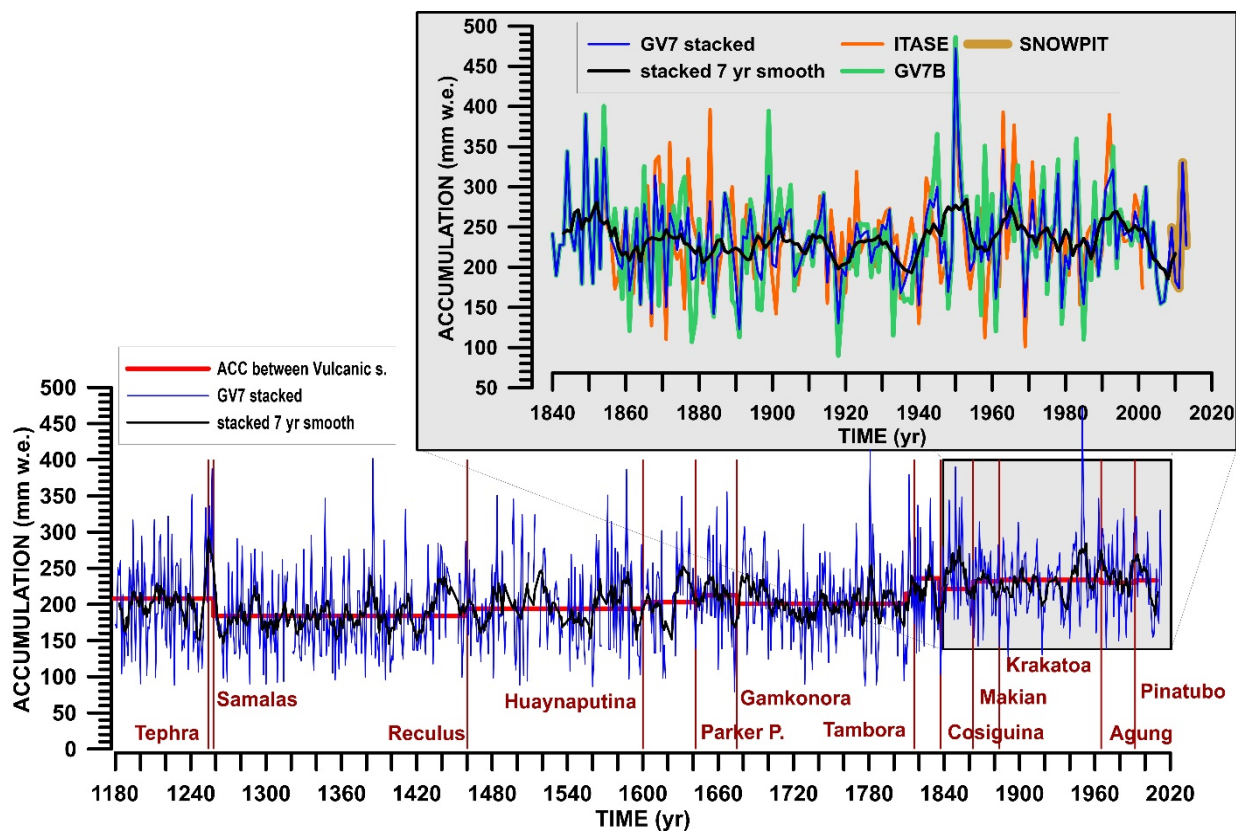
348 In order to remove the possible noise due to spatial variability (Frezzotti et al., 2007) and reduce the error connected to the
349 underestimating (overestimating) of the amount of yearly snow accumulated by misinterpreting the summer maxima in the
350 nssSO_4^{2-} profile, a stacked record was obtained by combination of trench (2013–2008 CE), GV7B core (2009–1079 CE),
351 stake measurements (2003–2001) and ITASE core (2001–1849 CE). The new stacked record (Figure 6) can give valuable
352 information on snow accumulation trend in the Antarctic region through comparison with other ice cores drilled in the same
353 sector. In the East Antarctic region, facing the Southern Indian Ocean, only three ice core records of snow accumulation
354 cover a period longer than three centuries: GV7 stacked (2013–1179 CE, this paper), Law Dome (2012 CE– 22 BCE, Roberts
355 et al., 2015) and Talos Dome (2010–1217 CE; Stenni et al., 2001 Thomas et al., 2017). Other cores (D66, GV5, GV2, HN)
356 have been drilled but their records cover less than 300 years (Frezzotti et al., 2013; Thomas et al., 2017). Precipitations over
357 the GV7 area are related to storms coming from the Southern Indian Ocean (Caiazzo et al., 2017) as for Law Dome, whereas
358 the precipitation at Talos Dome coming only for 50% from Southern Indian Ocean and the remaining from the Ross Sea
359 (Sodemann and Stohl, 2009; Scarchilli et al. 2011). Law Dome (DSS) is a site close to the Southern Ocean (100 km from the
360 shoreline) at about 1400 m of elevation with a long term of accumulation of 740 mm w.e. yr^{-1} (van Ommen et al., 2004),
361 about 1900 km west of GV7. Whereas Talos Dome is located at 2316 m and 250 km southern inland of GV7, with a long-
362 term accumulation of 80 mm w.e. yr^{-1} (Stenni et al., 2001). Roberts et al. (2015) pointed out that the two thousand years (22
363 BCE to 2012 CE) records at Law Dome shows no long-term trend in snow accumulation rates, however several anomalous
364 periods of accumulation exist in the record, most notably the periods of 380–442 CE, 727–783 CE and 1970–2009 CE (high
365 accumulation) and 663–704 CE, 933– 975 CE and 1429–1468 CE (low accumulation). Law Dome accumulation variability
366 is associated with both ENSO and IPO (Roberts et al., 2015; Vance et al., 2015), which influence the meridional component
367 of the large-scale circulation (van Ommen and Morgan, 2010; Roberts et al., 2015; Vance et al., 2015). For Talos Dome,
368 Stenni et al., (2001) pointed out for the period 1996–1217 CE a decrease during part of the Little Ice Age followed by an
369 increment of about 11% in accumulation during the 20th century.



370 The comparative analysis of the last 800 years of these three records shows a significant trend in accumulation record at
371 GV7 and Law Dome (Table 3), with a high increase in accumulated snow in the former and a slight increase in the latter (47
372 and 20 mm w.e., ~23% and ~2% of the mean accumulation over 800 years, respectively). On the other hand, no significant
373 trend at Talos Dome is apparent (Table 3).

374 Our analysis of variability at multi-centennial scale shows for GV7 a decrease of the accumulation rate from the beginning
375 of the record (1200 CE) to the middle of the 14th century. An analogous decrease has been already observed at Law Dome
376 (Roberts et al., 2015) and at Talos Dome (Stenni et al. 2001) (Figure 7). An increase in accumulation up to now is present at
377 GV7 and Talos Dome starting around middle 18th century (Table 3), whereas at Law Dome the data shows an increase a
378 century later from middle of 19th century. Decadal-scale snow accumulation anomalies were found at Law Dome to be
379 relatively common (74 events in the 2035-year record; Roberts et al., 2015). The previous study regarding the Talos Dome –
380 GV7 area, pointed out a century-scale variability with slight increase (of a few percent) in accumulation rates over the last
381 200 years, in particular since the 1960s, compared with the period 1816– 1965 CE (Frezzotti et al., 2007, 2013). At GV7 the
382 observed increase in accumulation during the last 250 years is greater than the observed range for the previous 600 years
383 (Figure 7). Frezzotti et al., 2013 analyzed 67 records from the entire continent over the last 800 yr to assess the temporal
384 variability of accumulation rates. The temporal and spatial variability of the records over the previous 800 yr indicates that
385 snow accumulation changes over most of Antarctica are statistically negligible and do not exhibit an overall long clear trend.
386 However, a clear increase in accumulation of more than 10% has observed in coastal and slope regions, as also this record
387 shows for GV7 site. Thomas et al., 2017 reveals that snow accumulation for the total Antarctica has increased since 1800
388 AD, where the annual snow accumulation during the most recent decade (2001–2010) is higher than the annual average at
389 the start of the 19th century. The Antarctic Peninsula is the only region where both the most recent 50- and 100- year trends
390 are greater than of the observed range for the past 300 years.

391
392
393
394

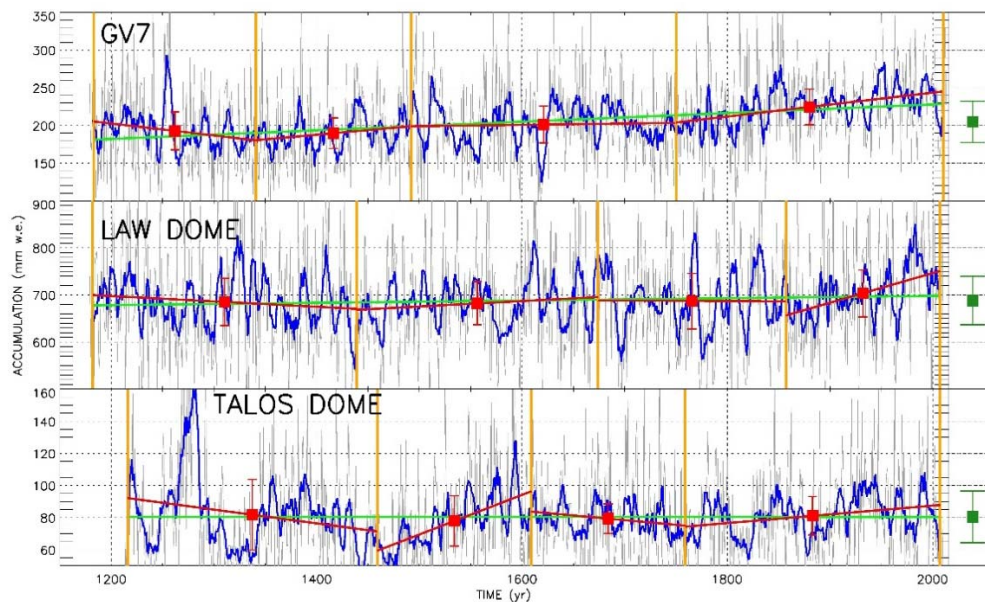


395

396 Figure 6: a) Time series from 1840 to 2020 CE of the GV7 snowpit trench (2013-2008 CE, gold line); the ITASE core (2001-1849
 397 CE, orange line) and the GV7 B core (2009-1179 CE, green line). Blue and black lines highlight the stacked record, obtained
 398 coupling the snowpit, ITASE and GV7 B core, and its smoothing at 7 years, respectively. b) GV7 stacked complete time record
 399 (1179-2013 CE) with seven years smoothing average (black line). Red vertical bars highlight volcanic eruption horizon and red line
 400 shows average accumulation between different volcanic events.

401

402



403

404 **Figure 7: a) GV7 stacked record (gray line) with its seven years smoothing average (blue line); green line represents trend for the**
405 **1179-2013 CE record. Yellow vertical bars show breaking points (1183 CE, 1341 CE, 1492 CE, 1750 CE and 2010 CE) calculated**
406 **following Tomé and Miranda (2004). Red lines and filled squares show partial trends and mean accumulation (with standard**
407 **deviation error bars) for each sub-period defined by breaking points. Green filled square with error bar highlights mean**
408 **accumulation at the site and its standard deviation, respectively, for the whole period (1179-2013 CE). b) Same as A but for Law**
409 **Dome ice core for the period 1179-2013 CE with breaking points at 1182 CE, 1439 CE, 1674 CE, 1857 CE and 2007 CE. c) Same as**
410 **A but for Talos Dome ice core for the period 1216-2010 CE with breaking points at 1216 CE, 1459 CE, 1609 CE, 1759 CE and 2007**
411 **CE.**



412

GV7	1183-2010 Tr=+0.6 (p < 0.001) M=205 SD=27	1183-1341 Tr=-1.6 (p < 0.001) M=193 SD=25	1341-1492 Tr=1.2 (p < 0.001) M=190 SD=20	1492-1750 Tr=0.2 (No sign.) M=201 SD=24	1750-2010 Tr=1.6 (p < 0.001) M=224 SD=24
	LAW DOME	1183-2007 Tr=-0.3 (p < 0.001) M=688 SD=52	1183-1439 Tr=-1.1 (p < 0.01) M=685 SD=50	1439-1674 Tr=1.1 (p < 0.01) M=682 SD=46	1674-1857 Tr=-0.1 (No sign) M=687 SD=59
TALOS DOME	1216 -1996 No trend M=80 SD=16	1217-1459 Tr=-0.9 (p < 0.001) M=82 SD=22	1459-1609 Tr=2.5 (p < 0.001) M=78 SD=16	1609-1759 Tr=-0.6 (p < 0.001) M=79 SD=9	1759-2007 Tr=0.5 (p < 0.001) M=81 SD=12

413

414 **Table 3: Values of trend with significance (Tr, mm w.e./decade), mean accumulation and its standard deviation (M and Sd,**
 415 **respectively; mm w.e. yr-1) for GV7 stacked, Law Dome and Talos Dome smoothed with a 7-year running average, within**
 416 **different period defined by breaking points calculated following Tomé and Miranda (2004).**

417 **4 Conclusion**

418 In this work, we used the chemical stratigraphies obtained from the analysis of about 3500 discrete samples from the
 419 GV7(B) ice core to accurately date the core with a sub-annual resolution. $\delta^{18}\text{O}$ high resolution record was compared to
 420 nssSO_4^{2-} profile showing negligible discrepancies. The two records were used to achieve a reliable dating of the uppermost
 421 section of the core (approx. 40m, covering the time period between 2009 and 1920 CE).

422 For the deeper section of the core, different strategies were tested and compared, namely single-parameter and multi-
 423 parametric approaches by considering seasonal markers to accomplish an annual layer counting. Upon these tests, nssSO_4^{2-}
 424 profile was chosen for the dating of the core because of its clearer and better-preserved seasonal pattern all along the ice
 425 core, even at higher depth, where the temporal resolution becomes lower due to the thinning of the ice layers. An accurate
 426 annual layer counting was applied, and the volcanic signatures identified in the GV7 ice core were used as temporal horizons



427 and tie points in the dating procedure. In this way, an accurate dating of the core with a sub-annual resolution for the
428 uppermost 197 m was obtained.. Unfortunately, beyond the depth of 197 m, the ice core was strongly damaged and thus
429 heavily contaminated from the drilling fluid also in the inner part.

430 The time period covered by this uppermost 197 m of the core resulted to be 1179 - 2009 CE. In this period, an average
431 annual snow accumulation rate of 205 mm w.e. was calculated. Such value was compared with already available records
432 from the same site and different cores drilled in the same region (Law Dome and Talos Dome). Similar accumulation rate
433 was found when comparing it with another core drilled on the same site as part of the ITASE drilling campaign, with
434 particularly good agreement during the last 40 years. When considering the general trend of the accumulation throughout the
435 years, an increase was found since middle 18th century covered by the GV7(B) core. Such increasing trend has been
436 observed also at other slope coastal sites. Although the data here presented only cover the last 830 years, the number of cores
437 that cover the same time period is still scarce, therefore the present study could significantly contribute to the long-term
438 assessment of the surface mass balance in this area.

439 **5 Acknowledgment**

440 This research was financially supported by the MIUR (Italian Ministry of University and Research) - PNRA (Italian
441 Antarctic Research Programme) through the IPICS-2kyr-It project (International Partnership for Ice Core Science,
442 reconstructing the climate variability for the last 2kyr, the Italian contribution). The IPICS-2kyr-It project is carried out in
443 cooperation with KOPRI (Korea Polar Research Institute, grant No. PE21100).

444 The fellowship personnel involved in the analysis of the GV7 core, and the laboratory equipment was partially funded by
445 Fondazione Cassa di Risparmio di Firenze, MIUR-PNRA IPICS-2kyr-Italia (PNRA 2009/A2.09) MIUR-PNRA “BE-OI”
446 (PNRA16 00124) and “3D” (PNRA16 00212) projects and MIUR-PRIN 2017 “AMICO”.

447 **6 References**

448 Abram, N. J., Wolff, E. W. and Curran, M. A. J.: A review of sea ice proxy information from polar ice cores, *Quaternary*
449 *Science Reviews*, 79, 168–183, <https://doi.org/10.1016/j.quascirev.2013.01.011>, 2013.

450 Alley, R. B., Shuman, C. A., Meese, D. A., Gow, A. J., Taylor, K. C., Cuffey, K. M., Fitzpatrick, J. J., Grootes, P. M.,
451 Zielinski, G. A., Ram, M., Spinelli, G. and Elder, B.: Visual-stratigraphic dating of the GISP2 ice core: Basis,
452 reproducibility, and application, *Journal of Geophysical Research: Oceans*, 102(C12), 26367–26381,
453 <https://doi.org/10.1029/96JC03837>, 1997.

454 Becagli, S., Proposito, M., Benassai, S., Flora, O., Genoni, L., Gragnani, R., Largiuni, O., Pili, S. L., Severi, M., Stenni, B.,
455 Traversi, R., Udisti, R. and Frezzotti, M.: Chemical and isotopic snow variability in East Antarctica along the 2001/02
456 ITASE traverse, *Annals of Glaciology*, 39, 473–482, <https://doi.org/10.3189/172756404781814636>, 2004.



- 457 Becagli, S., Scarchilli, C., Traversi, R., Dayan, U., Severi, M., Frosini, D., Vitale, V., Mazzola, M., Lupi, A., Nava, S. and
458 Udisti, R.: Study of present-day sources and transport processes affecting oxidised sulphur compounds in atmospheric
459 aerosols at Dome C (Antarctica) from year-round sampling campaigns, *Atmospheric Environment*, 52, 98–108,
460 <https://doi.org/10.1016/j.atmosenv.2011.07.053>, 2012.
- 461 Benassai, S., Becagli, S., Gragnani, R., Magand, O., Proposito, M., Fattori, I., Traversi, R. and Udisti, R.: Sea-spray
462 deposition in Antarctic coastal and plateau areas from ITASE traverses, *Annals of Glaciology*, 41, 32–40,
463 <https://doi.org/10.3189/172756405781813285>, 2005.
- 464 Bertler, N. A. N., Mayewski, P. A. and Carter, L.: Cold conditions in Antarctica during the Little Ice Age - Implications for
465 abrupt climate change mechanisms, *Earth and Planetary Science Letters*, 308(1–2), 41–51,
466 <https://doi.org/10.1016/j.epsl.2011.05.021>, 2011.
- 467 Bodhaine, B. A., Deluisi, J. J., Harris, J. M., Houmère, P. and Bauman, S.: Aerosol measurements at the South Pole, *Tellus*
468 B, 38 B(3–4), 223–235, <https://doi.org/10.1111/j.1600-0889.1986.tb00189.x>, 1986.
- 469 Bowen, H. J. M.: *Environmental chemistry of the elements*, Academic Press, London., 1979.
- 470 Caiazza, L., Becagli, S., Frosini, D., Giardi, F., Severi, M., Traversi, R. and Udisti, R.: Spatial and temporal variability of
471 snow chemical composition and accumulation rate at Talos Dome site (East Antarctica), *Science of the Total Environment*,
472 550, 418–430, <https://doi.org/10.1016/j.scitotenv.2016.01.087>, 2016.
- 473 Caiazza, L., Baccolo, G., Barbante, C., Becagli, S., Bertò, M., Ciardini, V., Crotti, I., Delmonte, B., Dreossi, G., Frezzotti,
474 M., Gabrieli, J., Giardi, F., Han, Y., Hong, S. B., Hur, S. D., Hwang, H., Kang, J. H., Narcisi, B., Proposito, M., Scarchilli,
475 C., Selmo, E., Severi, M., Spolaor, A., Stenni, B., Traversi, R. and Udisti, R.: Prominent features in isotopic, chemical and
476 dust stratigraphies from coastal East Antarctic ice sheet (Eastern Wilkes Land), *Chemosphere*, 176, 273–287,
477 <https://doi.org/10.1016/j.chemosphere.2017.02.115>, 2017.
- 478 Candelone, J.-P., Hong, S. and Boutron, C. F.: An improved method for decontaminating polar snow or ice cores for heavy
479 metal analysis, *Analytica Chimica Acta*, 299(1), 9–16, 1994.
- 480 Candelone, J.-P., Bolshov, M. A., Rudniev, S. N., Hong, S. and Boutron, C. F.: Bismuth in recent snow from Central
481 Greenland: Preliminary results, *Atmospheric Environment*, 29(15), [https://doi.org/10.1016/1352-2310\(95\)00058-7](https://doi.org/10.1016/1352-2310(95)00058-7), 1995.
- 482 Castellano, E., Becagli, S., Jouzel, J., Migliori, A., Severi, M., Steffensen, J. P., Traversi, R. and Udisti, R.: Volcanic
483 eruption frequency over the last 45 ky as recorded in Epica-Dome C ice core (East Antarctica) and its relationship with
484 climatic changes, in *Global and Planetary Change*, vol. 42, pp. 195–205, <https://doi.org/10.1016/j.gloplacha.2003.11.007>,
485 2004.
- 486 Castellano, E., Becagli, S., Hansson, M., Hutterli, M., Petit, J. R., Rampino, M. R., Severi, M., Steffensen, J. P., Traversi, R.
487 and Udisti, R.: Holocene volcanic history as recorded in the sulfate stratigraphy of the European Project for Ice Coring in
488 Antarctica Dome C (EDC96) ice core, *Journal of Geophysical Research D: Atmospheres*, 110(6), 1–12,
489 <https://doi.org/10.1029/2004JD005259>, 2005.



- 490 Chisholm, W., Rosman, K. J. R., Boutron, C. F., Candelone, J. P. and Hong, S.: Determination of lead isotopic ratios in
491 Greenland and Antarctic snow and ice at picogram per gram concentrations, *Analytica Chimica Acta*, 311(2), 141–151,
492 [https://doi.org/10.1016/0003-2670\(95\)00181-X](https://doi.org/10.1016/0003-2670(95)00181-X), 1995.
- 493 Cole-Dai, J., Mosley-Thompson, E. and Thompson, L. G.: Annually resolved southern hemisphere volcanic history from two
494 Antarctic ice cores, *Journal of Geophysical Research Atmospheres*, 102(14), 16761–16771,
495 <https://doi.org/10.1029/97jd01394>, 1997.
- 496 Dansgaard, W.: Stable isotopes in precipitation, *Tellus*, 16(4), 436–468, <https://doi.org/10.1111/j.2153-3490.1964.tb00181.x>,
497 1964.
- 498 DeConto, R. M. and Pollard, D.: Contribution of Antarctica to past and future sea-level rise, *Nature*, 531(7596),
499 <https://doi.org/10.1038/nature17145>, 2016.
- 500 Delmas, R. J., Legrand, M., Aristarain, A. J. and Zanolini, F.: Volcanic deposits in Antarctic snow and ice., *Journal of*
501 *Geophysical Research*, 90(D7), 12901–12920, <https://doi.org/10.1029/JD090iD07p12901>, 1985.
- 502 Delmonte, B., Petit, J. and Maggi, V.: Glacial to Holocene implications of the new 27000-year dust record from the EPICA
503 Dome C (East Antarctica) ice core, *Climate Dynamics*, 18(8), 647–660, <https://doi.org/10.1007/s00382-001-0193-9>, 2002.
- 504 Delmonte, B., Giovanni, B., Fausto, M., Iizuka, Y. and Valter, M.: Dust flux in peripheral East Antarctica: preliminary
505 results from GV7 ice core and extension of the TALDICE dust record to the sub-micron range., 2015.
- 506 Dibb, J. E., Talbot, R. W., Munger, J. W., Jacob, D. J. and Fan, S. M.: Air-snow exchange of HNO₃ and NO_y at Summit,
507 Greenland, *Journal of Geophysical Research Atmospheres*, 103(D3), 3475–3486, <https://doi.org/10.1029/97JD03132>, 1998.
- 508 Epstein, S. and Mayeda, T.: Variation of O₁₈ content of waters from natural sources, *Geochimica et Cosmochimica Acta*,
509 4(5), [https://doi.org/10.1016/0016-7037\(53\)90051-9](https://doi.org/10.1016/0016-7037(53)90051-9), 1953.
- 510 Erbland, J., Vicars, W. C., Savarino, J., Morin, S., Frey, M. M., Frosini, D., Vince, E. and Martins, J. M. F.: Air-snow
511 transfer of nitrate on the East Antarctic Plateau - Part 1: Isotopic evidence for a photolytically driven dynamic equilibrium in
512 summer, *Atmospheric Chemistry and Physics*, 13(13), 6403–6419, <https://doi.org/10.5194/acp-13-6403-2013>, 2013.
- 513 Extier, T., Landais, A., Bréant, C., Prié, F., Bazin, L., Dreyfus, G., Roche, D. M. and Leuenberger, M.: On the use of
514 $\delta^{18}\text{O}_{\text{atm}}$ for ice core dating, *Quaternary Science Reviews*, 185, 244–257, <https://doi.org/10.1016/j.quascirev.2018.02.008>,
515 2018.
- 516 Fischer, H., Fundel, F., Ruth, U., Twarloh, B., Wegner, A., Udisti, R., Becagli, S., Castellano, E., Morganti, A., Severi, M.,
517 Wolff, E., Littot, G., Röthlisberger, R., Mulvaney, R., Hutterli, M. A., Kaufmann, P., Federer, U., Lambert, F., Bigler, M.,
518 Hansson, M., Jonsell, U., de Angelis, M., Boutron, C., Siggaard-Andersen, M. L., Steffensen, J. P., Barbante, C., Gaspari,
519 V., Gabrielli, P. and Wagenbach, D.: Reconstruction of millennial changes in dust emission, transport and regional sea ice
520 coverage using the deep EPICA ice cores from the Atlantic and Indian Ocean sector of Antarctica, *Earth and Planetary*
521 *Science Letters*, 260(1–2), 340–354, <https://doi.org/10.1016/j.epsl.2007.06.014>, 2007.



- 522 Frezzotti, M., Urbini, S., Proposito, M., Scarchilli, C. and Gandolfi, S.: Spatial and temporal variability of surface mass
523 balance near Talos Dome, East Antarctica, *Journal of Geophysical Research: Earth Surface*, 112(2),
524 <https://doi.org/10.1029/2006JF000638>, 2007.
- 525 Frezzotti, M., Scarchilli, C., Becagli, S., Proposito, M. and Urbini, S.: A synthesis of the Antarctic surface mass balance
526 during the last 800 yr, *The Cryosphere*, 7(1), <https://doi.org/10.5194/tc-7-303-2013>, 2013.
- 527 Gondwe, M., Krol, M., Gieskes, W., Klaassen, W. and de Baar, H.: The contribution of ocean-leaving DMS to the global
528 atmospheric burdens of DMS, MSA, SO₂, and NSS SO₄, *Global Biogeochemical Cycles*, 17(2), n/a-n/a,
529 <https://doi.org/10.1029/2002gb001937>, 2003.
- 530 Grannas, A. M., Jones, A. E., Dibb, J., Ammann, M., Anastasio, C., Beine, H. J., Bergin, M., Bottenheim, J., Boxe, C. S.,
531 Carver, G., Chen, G., Crawford, J. H., Dominé, F., Frey, M. M., Guzmán, M. I., Heard, D. E., Helmig, D., Hoffmann, M. R.,
532 Honrath, R. E., Huey, L. G., Hutterli, M., Jacobi, H. W., Klán, P., Lefér, B., McConnell, J., Plane, J., Sander, R., Savarino, J.,
533 Shepson, P. B., Simpson, W. R., Sodeau, J. R., von Glasow, R., Weller, R., Wolff, E. W. and Zhu, T.: An overview of snow
534 photochemistry: evidence, mechanisms and impacts, *Atmospheric Chemistry and Physics*, 7(16), 4329–4373, 2007.
- 535 Hammer, C. U.: Acidity of Polar Ice Cores in Relation to Absolute Dating, Past Volcanism, and Radio–Echoes, *Journal of*
536 *Glaciology*, 25(93), 359–372, 1980.
- 537 Hastings, M. G., Sigman, D. M. and Steig, E. J.: Glacial/interglacial changes in the isotopes of nitrate from the Greenland Ice
538 Sheet Project 2 (GISP2) ice core, *Global Biogeochemical Cycles*, 19(4), <https://doi.org/10.1029/2005GB002502>, 2005.
- 539 Herron, M. M. and Langway, C. C.: Dating of Ross Ice Shelf Core by chemical analysis, *Journal of Glaciology*, 24(90),
540 1979.
- 541 Hwang, H., Hur, S. do, Lee, J., Han, Y., Hong, S. and Motoyama, H.: Plutonium fallout reconstructed from an Antarctic
542 Plateau snowpack using inductively coupled plasma sector field mass spectrometry, *Science of the Total Environment*, 669,
543 505–511, <https://doi.org/10.1016/j.scitotenv.2019.03.105>, 2019.
- 544 Igarashi, M., Nakai, Y., Motizuki, Y., Takahashi, K., Motoyama, H. and Makishima, K.: Dating of the Dome Fuji shallow
545 ice core based on a record of volcanic eruptions from AD 1260 to AD 2001, *Polar Science*, 5(4), 411–420,
546 <https://doi.org/10.1016/j.polar.2011.08.001>, 2011.
- 547 Jiang, S., Shi, G., Cole-Dai, J., Geng, L., Ferris, D. G., An, C. and Li, Y.: Nitrate preservation in snow at Dome A, East
548 Antarctica from ice core concentration and isotope records, *Atmospheric Environment*, 213, 405–412,
549 <https://doi.org/10.1016/j.atmosenv.2019.06.031>, 2019.
- 550 Jones, J. M., Gille, S. T., Goosse, H., Abram, N. J., Canziani, P. O., Charman, D. J., Clem, K. R., Crosta, X., de Lavergne,
551 C., Eisenman, I., England, M. H., Fogt, R. L., Frankcombe, L. M., Marshall, G. J., Masson-Delmotte, V., Morrison, A. K.,
552 Orsi, A. J., Raphael, M. N., Renwick, J. A., Schneider, D. P., Simpkins, G. R., Steig, E. J., Stenni, B., Swingedouw, D. and
553 Vance, T. R.: Assessing recent trends in high-latitude Southern Hemisphere surface climate, *Nature Climate Change*, 6(10),
554 917–926, <https://doi.org/10.1038/nclimate3103>, 2016.



- 555 Kellerhals, T., Tobler, L., Brüttsch, S., Sigl, M., Wacker, L., Gäggeler, H. W. and Schwikowski, M.: Thallium as a Tracer for
556 Preindustrial Volcanic Eruptions in an Ice Core Record from Illimani, Bolivia, *Environmental Science & Technology*, 44(3),
557 <https://doi.org/10.1021/es902492n>, 2010.
- 558 Krinner, G., Magand, O., Simmonds, I., Genthon, C. and Dufresne, J. L.: Simulated Antarctic precipitation and surface mass
559 balance at the end of the twentieth and twenty-first centuries, *Climate Dynamics*, 28(2–3), 215–230,
560 <https://doi.org/10.1007/s00382-006-0177-x>, 2007.
- 561 Legrand, M., Wolff, E. and Wagenbach, D.: Antarctic aerosol and snowfall chemistry: implications for deep Antarctic ice-
562 core chemistry, *Annals of Glaciology*, 29, 66–72, 1999.
- 563 Legrand, M. R. and Delmas, R. J.: The ionic balance of Antarctic snow: A 10-year detailed record, *Atmospheric*
564 *Environment*, 18(9), 1867–1874, 1984.
- 565 Magand, O., Frezzotti, M., Pourchet, M., Stenni, B., Genoni, L. and Fily, M.: Climate variability along latitudinal and
566 longitudinal transects in East Antarctica., *Annals of Glaciology*, 39, 351–358, 2004.
- 567 Maupetit, F. and Delmas, R. J.: Chemical composition of Falling Snow at Dumont D’Urville, Antarctica, *Journal of*
568 *Atmospheric Chemistry*, 14, 31–42, 1992.
- 569 Morganti, A., Becagli, S., Castellano, E., Severi, M., Traversi, R. and Udisti, R.: An improved flow analysis-ion
570 chromatography method for determination of cationic and anionic species at trace levels in Antarctic ice cores, *Analytica*
571 *Chimica Acta*, 603(2), 190–198, <https://doi.org/10.1016/j.aca.2007.09.050>, 2007.
- 572 Mulvaney, R. and Wolff, E. W.: Spatial variability of the major chemistry of the Antarctic ice sheet, *Annals of Glaciology*,
573 20, 440–447, <https://doi.org/10.3189/1994aog20-1-440-447>, 1994.
- 574 Narcisi, B. and Petit, J. R.: *Englacial tephros of East Antarctica*, edited by J. Smellie, K. Panter, and A. Geyer, Geological
575 Society, London, 2021.
- 576 Narcisi, B., Proposito, M. and Frezzotti, M.: Ice record of a 13th century explosive volcanic eruption in northern Victoria
577 Land, East Antarctica, *Antarctic Science*, 13(2), 174–181, <https://doi.org/10.1017/S0954102001000268>, 2001.
- 578 Narcisi, B., Petit, J. R., Delmonte, B., Scarchilli, C. and Stenni, B.: A 16,000-yr tephra framework for the Antarctic ice sheet:
579 A contribution from the new Talos Dome core, *Quaternary Science Reviews*, 49, 52–63,
580 <https://doi.org/10.1016/j.quascirev.2012.06.011>, 2012.
- 581 Nardin, R., Amore, A., Becagli, S., Caiazzo, L., Frezzotti, M., Severi, M., Stenni, B. and Traversi, R.: Volcanic Fluxes Over
582 the Last Millennium as Recorded in the Gv7 Ice Core (Northern Victoria Land, Antarctica), *Geosciences*, 10(1), 38,
583 <https://doi.org/10.3390/geosciences10010038>, 2020.
- 584 Neukom, R., Schurer, A. P., Steiger, Nathan. J. and Hegerl, G. C.: Possible causes of data model discrepancy in the
585 temperature history of the last Millennium, *Scientific Reports*, 8(1), 7572, <https://doi.org/10.1038/s41598-018-25862-2>,
586 2018.
- 587 Nozaki, Y.: A fresh look at element distribution in the North Pacific Ocean, *Eos*, 78(21), 221,
588 <https://doi.org/10.1029/97eo00148>, 1997.



- 589 Nyamangerel, Y., Han, Y., Kim, S., Hong, S.-B., Lee, J. and Hur, S. do: Chronological characteristics for snow accumulation
590 on Styx Glacier in northern Victoria Land, Antarctica, *Journal of Glaciology*, 1–11, <https://doi.org/10.1017/jog.2020.53>,
591 2020.
- 592 Pasteris, D. R., McConnell, J. R., Das, S. B., Criscitiello, A. S., Evans, M. J., Maselli, O. J., Sigl, M. and Layman, L.:
593 Seasonally resolved ice core records from West Antarctica indicate a sea ice source of sea-salt aerosol and a biomass burning
594 source of ammonium, *Journal of Geophysical Research*, 119(14), 9168–9182, <https://doi.org/10.1002/2013JD020720>, 2014.
- 595 Piccardi, G., Udisti, R. and Casella, F.: Seasonal trends and chemical composition of snow at terra nova bay (antarctica),
596 *International Journal of Environmental Analytical Chemistry*, 55(1–4), 219–234,
597 <https://doi.org/10.1080/03067319408026220>, 1994.
- 598 Rasmussen, S. O., Andersen, K. K., Svensson, A. M., Steffensen, J. P., Vinther, B. M., Clausen, H. B., Siggaard-Andersen,
599 M. L., Johnsen, S. J., Larsen, L. B., Dahl-Jensen, D., Bigler, M., Röthlisberger, R., Fischer, H., Goto-Azuma, K., Hansson,
600 M. E. and Ruth, U.: A new Greenland ice core chronology for the last glacial termination, *Journal of Geophysical Research*
601 *Atmospheres*, 111(6), <https://doi.org/10.1029/2005JD006079>, 2006.
- 602 Roberts, J., Plummer, C., Vance, T., van Ommen, T., Moy, A., Poynter, S., Treverrow, A., Curran, M. and George, S.: A
603 2000-year annual record of snow accumulation rates for Law Dome, East Antarctica, *Climate of the Past*, 11(5), 697–707,
604 2015.
- 605 Röthlisberger, R., Hutterli, M. A., Sommer, S., Wolff, E. W. and Mulvaney, R.: Factors controlling nitrate in ice cores:
606 Evidence from the Dome C deep ice core, *Journal of Geophysical Research Atmospheres*, 105(D16), 20565–20572,
607 <https://doi.org/10.1029/2000JD900264>, 2000.
- 608 Röthlisberger, R., Hutterli, M. A., Wolff, E. W., Mulvaney, R., Fischer, H., Bigler, M., Goto-Azuma, K., Hansson, M. E.,
609 Ruth, U., Siggaard-Andersen, M.-L. and Steffensen, J. P.: Nitrate in Greenland and Antarctic ice cores: a detailed description
610 of post-depositional processes, *Annals of Glaciology*, 35, 209–216, 2002.
- 611 Scarchilli, C., Frezzotti, M. and Ruti, P. M.: Snow precipitation at four ice core sites in East Antarctica: provenance,
612 seasonality and blocking factors, *Climate Dynamics*, 37(9–10), 2107–2125, <https://doi.org/10.1007/s00382-010-0946-4>,
613 2011.
- 614 Severi, M., Becagli, S., Castellano, E., Morganti, A., Traversi, R., Udisti, R., Ruth, U., Fischer, H., Huybrechts, P., Wolff,
615 E., Parrenin, F., Kaufmann, P., Lambert, F. and Steffensen, J. P.: Synchronisation of the EDML and EDC ice cores for the
616 last 52 kyr by volcanic signature matching, *Climate of the Past*, 3(3), 367–374, <https://doi.org/10.5194/cp-3-367-2007>, 2007.
- 617 Severi, M., Udisti, R., Becagli, S., Stenni, B. and Traversi, R.: Volcanic synchronisation of the EPICA-DC and TALDICE
618 ice cores for the last 42 kyr BP, *Climate of the Past*, 8(2), 509–517, <https://doi.org/10.5194/cp-8-509-2012>, 2012.
- 619 Sigl, M., McConnell, J. R., Layman, L., Maselli, O., McGwire, K., Pasteris, D., Dahl-Jensen, D., Steffensen, J. P., Vinther,
620 B., Edwards, R., Mulvaney, R. and Kipfstuhl, S.: A new bipolar ice core record of volcanism from WAIS Divide and NEEM
621 and implications for climate forcing of the last 2000 years, *Journal of Geophysical Research Atmospheres*, 118(3), 1151–
622 1169, <https://doi.org/10.1029/2012JD018603>, 2013.



- 623 Sigl, M., Winstrup, M., McConnell, J. R., Welten, K. C., Plunkett, G., Ludlow, F., Büntgen, U., Caffee, M., Chellman, N.,
624 Dahl-Jensen, D., Fischer, H., Kipfstuhl, S., Kostick, C., Maselli, O. J., Mekhaldi, F., Mulvaney, R., Muscheler, R., Pasteris,
625 D. R., Pilcher, J. R., Salzer, M., Schüpbach, S., Steffensen, J. P., Vinther, B. M. and Woodruff, T. E.: Timing and climate
626 forcing of volcanic eruptions for the past 2,500 years, *Nature*, 523(7562), 543–549, <https://doi.org/10.1038/nature14565>,
627 2015.
- 628 Sigl, M., Fudge, T. J., Winstrup, M., Cole-Dai, J., Ferris, D., McConnell, J. R., Taylor, K. C., Welten, K. C., Woodruff, T.
629 E., Adolphi, F., Bisiaux, M., Brook, E. J., Buizert, C., Caffee, M. W., Dunbar, N. W., Edwards, R., Geng, L., Iverson, N.,
630 Koffman, B., Layman, L., Maselli, O. J., McGwire, K., Muscheler, R., Nishiizumi, K., Pasteris, D. R., Rhodes, R. H. and
631 Sowers, T. A.: The WAIS Divide deep ice core WD2014 chronology - Part 2: Annual-layer counting (0–31 ka BP), *Climate*
632 *of the Past*, 12(3), 769–786, <https://doi.org/10.5194/cp-12-769-2016>, 2016.
- 633 Sodemann, H. and Stohl, A.: Asymmetries in the moisture origin of Antarctic precipitation, *Geophysical Research Letters*,
634 36(22), <https://doi.org/10.1029/2009GL040242>, 2009.
- 635 Stefels, J., Steinke, M., Turner, S., Malin, G. and Belviso, S.: Environmental constraints on the production and removal of
636 the climatically active gas dimethylsulphide (DMS) and implications for ecosystem modelling, in *Biogeochemistry*, 83, 245–
637 275, <https://doi.org/10.1007/s10533-007-9091-5>, 2007.
- 638 Stenni, B., Masson-Delmotte, V., Johnsen, S. J., Jouzel, J., Longinelli, A., Monnin, E., Rothlisberger, R., Selmo, E.: An
639 Oceanic Cold Reversal During the Last Deglaciation, *Science*, 293(5537), 2074–2077, 2001
- 640 Stenni, B., Proposito, M., Gragnani, R., Flora, O., Jouzel, J., Falourd, S. and Frezzotti, M.: Eight centuries of volcanic signal
641 and climate change at Talos Dome (East Antarctica), *Journal of Geophysical Research D: Atmospheres*, 107(9–10), 3–1,
642 <https://doi.org/10.1029/2000jd000317>, 2002.
- 643 Tao, G., Yamada, R., Fujikawa, Y., Kudo, A., Zheng, J., Fisher, D. A. and Koerner, R. M.: Determination of trace amounts
644 of heavy metals in arctic ice core samples using inductively coupled plasma mass spectrometry.
645 www.elsevier.com/locate/talanta, 2001.
- 646 Thomas, E. R., Wolff, E. W., Mulvaney, R., Steffensen, J. P., Johnsen, S. J., Arrowsmith, C., White, J. W. C., Vaughn, B.
647 and Popp, T.: The 8.2 ka event from Greenland ice cores, *Quaternary Science Reviews*, 26(1–2), 70–81,
648 <https://doi.org/10.1016/j.quascirev.2006.07.017>, 2007.
- 649 Thomas, E. R., Melchior Van Wessem, J., Roberts, J., Isaksson, E., Schlosser, E., Fudge, T. J., Vallelonga, P., Medley, B.,
650 Lenaerts, J., Bertler, N., van den Broeke, M. R., Dixon, D. A., Frezzotti, M., Stenni, B., Curran, M. and Ekaykin, A. A.:
651 Regional Antarctic snow accumulation over the past 1000 years, *Climate of the Past*, 13(11), 1491–1513,
652 <https://doi.org/10.5194/cp-13-1491-2017>, 2017.
- 653 Tomé, A., and Miranda, P. M. A.: Piecewise linear fitting and trend changing points of climate parameters, *Geophysical*
654 *Research Letters*, 31(2), L02207, doi:10.1029/2003GL019100, 2004



- 655 Traufetter, F., Oerter, H., Fischer, H., Weller, R. and Miller, H.: Spatio-temporal variability in volcanic sulphate deposition
656 over the past 2 kyr in snow pits and firn cores from Amundsenisen, Antarctica, *Journal of Glaciology*, 50(168), 137-146,
657 2004.
- 658 Traversi, R., Usoskin, I. G., Solanki, S. K., Becagli, S., Frezzotti, M., Severi, M., Stenni, B. and Udisti, R.: Nitrate in Polar
659 Ice: A New Tracer of Solar Variability, *Solar Physics*, 280(1), 237–254, <https://doi.org/10.1007/s11207-012-0060-3>, 2012.
- 660 Udisti, R.: Multiparametric approach for chemical dating of snow layers from Antarctica, *International Journal of*
661 *Environmental Analytical Chemistry*, 63(3), 225–244, <https://doi.org/10.1080/03067319608026268>, 1996.
- 662 Udisti, R., Dayan, U., Becagli, S., Busetto, M., Frosini, D., Legrand, M., Lucarelli, F., Preunkert, S., Severi, M., Traversi, R.
663 and Vitale, V.: Sea spray aerosol in central Antarctica. Present atmospheric behaviour and implications for paleoclimatic
664 reconstructions, *Atmospheric Environment*, 52, 109–120, <https://doi.org/10.1016/j.atmosenv.2011.10.018>, 2012.
- 665 Van Ommen, T., Morgan, V., Curran, M., Declacial and Holocene changes in accumulation at Law Dome, East Antarctica,
666 *Annals of Glaciology*, 39, 359-365, 2004.
- 667 Van omen, T. and Morgan, V., Snowfall increase in coastal East Antarctica linked with southwest Western Australian
668 drought, *Nature Geoscience*, 3(4), 267-272, 2010.
- 669 Vance, T. R., Roberts, J. L., Plummer, C. T., Kiem, A. S., van Ommen, T. D.; Interdecadal Pacific variability and eastern
670 Australian megadroughts over the last millennium, *Geophysical Research Letters*, 42(1), 129-137, 2015.
- 671 Watanabe, O., Kamiyama, K., Motoyama, H., Fujii, Y., Shoji, H. and Satow, K.: The paleoclimate record in the ice core at
672 Dome Fuji station, East Antarctica., 1999.
- 673 Weller, R., Wagenbach, D., Legrand, M., Elsässer, C., Tian-Kunze, X. and König-Langlo, G.: Continuous 25-yr aerosol
674 records at coastal Antarctica - I: Inter-annual variability of ionic compounds links to climate indices, *Tellus, Series B:*
675 *Chemical and Physical Meteorology*, 63(5), 901–919, <https://doi.org/10.1111/j.1600-0889.2011.00542.x>, 2011.
- 676 Winski, D. A., Fudge, T. J., Ferris, D. G., Osterberg, E. C., Fegyveresi, J. M., Cole-Dai, J., Thundercloud, Z., Cox, T. S.,
677 Kreutz, K. J., Ortman, N., Buizert, C., Epifanio, J., Brook, E. J., Beaudette, R., Severinghaus, J., Sowers, T., Steig, E. J.,
678 Kahle, E. C., Jones, T. R., Morris, V., Aydin, M., Nicewonger, M. R., Casey, K. A., Alley, R. B., Waddington, E. D.,
679 Iverson, N. A., Dunbar, N. W., Bay, R. C., Souney, J. M., Sigl, M. and McConnell, J. R.: The SP19 chronology for the South
680 Pole Ice Core - Part 1: Volcanic matching and annual layer counting, *Climate of the Past*, 15(5), 1793–1808,
681 <https://doi.org/10.5194/cp-15-1793-2019>, 2019.
- 682 Wolff, E. W.: Nitrate in Polar Ice, in *Ice Core Studies of Global Biogeochemical Cycles*, Springer Berlin Heidelberg, Berlin,
683 Heidelberg, https://doi.org/10.1007/978-3-642-51172-1_10, , 1995.
- 684 Wolff, E. W.: Ice sheets and nitrogen., *Philosophical transactions of the Royal Society of London. Series B, Biological*
685 *sciences*, 368(1621), 20130127, <https://doi.org/10.1098/rstb.2013.0127>, 2013.
- 686 Wolff, E. W., Barbante, C., Becagli, S., Bigler, M., Boutron, C. F., Castellano, E., de Angelis, M., Federer, U., Fischer, H.,
687 Fundel, F., Hansson, M., Hutterli, M., Jonsell, U., Karlin, T., Kaufmann, P., Lambert, F., Littot, G. C., Mulvaney, R.,
688 Röthlisberger, R., Ruth, U., Severi, M., Siggaard-Andersen, M. L., Sime, L. C., Steffensen, J. P., Stocker, T. F., Traversi, R.,



- 689 Twarloh, B., Udisti, R., Wagenbach, D. and Wegner, A.: Changes in environment over the last 800,000 years from chemical
690 analysis of the EPICA Dome C ice core, *Quaternary Science Reviews*, 29(1–2), 285–295,
691 <https://doi.org/10.1016/j.quascirev.2009.06.013>, 2010.
- 692 Zielinski, G. A., Mayewski, P. A., David Meeker, L., Whitlow, S. and Twickler, M. S.: A 110,000-Yr Record of Explosive
693 Volcanism from the GISP2 (Greenland) Ice Core, *Quaternary Research* 45(2), 109-118, 1996.